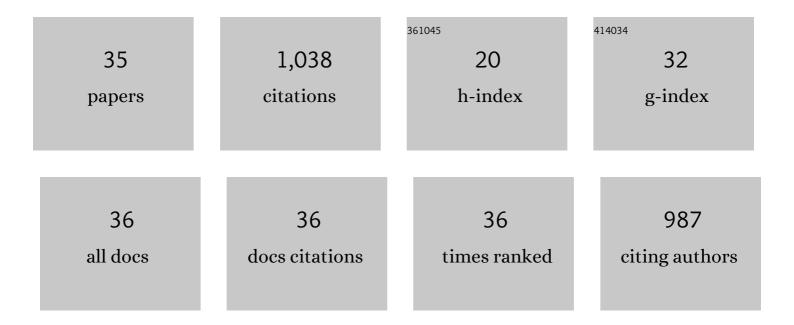
## **Ridong Wang**

List of Publications by Year in descending order

Source: https://exaly.com/author-pdf/5004741/publications.pdf

Version: 2024-02-01



| #  | Article  | IF  | CITATIONS |
|----|--|-----|-----------|
| 1  | Methods for Measuring Thermal Conductivity of Two-Dimensional Materials: A Review. Nanomaterials, 2022, 12, 589.   | 1.9 | 7         |
| 2  | Photothermal phenomenon: Extended ideas for thermophysical properties characterization. Journal of Applied Physics, 2022, 131, .   | 1.1 | 46        |
| 3  | DNA-Based Biosensors for the Biochemical Analysis: A Review. Biosensors, 2022, 12, 183.  | 2.3 | 32        |
| 4  | A Fiber-Based SPR Aptasensor for the In Vitro Detection of Inflammation Biomarkers. Micromachines, 2022, 13, 1036.   | 1.4 | 5         |
| 5  | A thermal activated and differential self-calibrated flexible epidermal biomicrofluidic device for wearable accurate blood glucose monitoring. Science Advances, 2021, 7, .  | 4.7 | 91        |
| 6  | Direct Characterization of Thermal Nonequilibrium between Optical and Acoustic Phonons in Graphene Paper under Photon Excitation. Advanced Science, 2021, 8, 2004712.  | 5.6 | 12        |
| 7  | The in-plane structure domain size of nm-thick MoSe <sub>2</sub> uncovered by low-momentum phonon scattering. Nanoscale, 2021, 13, 7723-7734.  | 2.8 | 7         |
| 8  | Interfacial Thermal Conductance between Monolayer WSe <sub>2</sub> and SiO <sub>2</sub> under<br>Consideration of Radiative Electron–Hole Recombination. ACS Applied Materials & Interfaces,<br>2020, 12, 51069-51081. | 4.0 | 18        |
| 9  | Energy and Charge Transport in 2D Atomic Layer Materials: Raman-Based Characterization.<br>Nanomaterials, 2020, 10, 1807.  | 1.9 | 8         |
| 10 | Thermal conductance between water and nm-thick WS <sub>2</sub> : extremely localized probing using nanosecond energy transport state-resolved Raman. Nanoscale Advances, 2020, 2, 5821-5832.                           | 2.2 | 6         |
| 11 | Distinguishing Optical and Acoustic Phonon Temperatures and Their Energy Coupling Factor under Photon Excitation in nm 2D Materials. Advanced Science, 2020, 7, 2000097.   | 5.6 | 34        |
| 12 | In situ investigation of annealing effect on thermophysical properties of single carbon nanocoil.<br>International Journal of Heat and Mass Transfer, 2020, 151, 119416.   | 2.5 | 15        |
| 13 | Pressure self-compensation for humidity sensing using graphene-oxide-modified dual-frequency CMUT.<br>Sensors and Actuators B: Chemical, 2020, 314, 128074.  | 4.0 | 2         |
| 14 | Thermal behavior of materials in laser-assisted extreme manufacturing: Raman-based novel characterization. International Journal of Extreme Manufacturing, 2020, 2, 032004.  | 6.3 | 25        |
| 15 | Thermal transport and energy dissipation in two-dimensional Bi2O2Se. Applied Physics Letters, 2019, 115, .   | 1.5 | 28        |
| 16 | Polarized Raman of Nanoscale Two-Dimensional Materials: Combined Optical and Structural Effects.<br>Journal of Physical Chemistry C, 2019, 123, 23236-23245.   | 1.5 | 16        |
| 17 | Hot carrier transfer and phonon transport in suspended nm WS2 films. Acta Materialia, 2019, 175, 222-237.  | 3.8 | 34        |
| 18 | Graphene Aerogel Based Bolometer for Ultrasensitive Sensing from Ultraviolet to Far-Infrared. ACS<br>Nano, 2019, 13, 5385-5396.  | 7.3 | 42        |

**RIDONG WANG** 

| #  | Article   | IF  | CITATIONS |
|----|---|-----|-----------|
| 19 | Anisotropic thermal conductivities and structure in lignin-based microscale carbon fibers. Carbon, 2019, 147, 58-69.  | 5.4 | 37        |
| 20 | Frequency-domain energy transport state-resolved Raman for measuring the thermal conductivity of suspended nm-thick MoSe2. International Journal of Heat and Mass Transfer, 2019, 133, 1074-1085.                       | 2.5 | 48        |
| 21 | Thermal conductivity of SiC microwires: Effect of temperature and structural domain size uncovered by 0 K limit phonon scattering. Ceramics International, 2018, 44, 11218-11224.                                       | 2.3 | 25        |
| 22 | Very fast hot carrier diffusion in unconstrained MoS <sub>2</sub> on a glass substrate: discovered by picosecond ET-Raman. RSC Advances, 2018, 8, 12767-12778.  | 1.7 | 24        |
| 23 | Characterization of anisotropic thermal conductivity of suspended nm-thick black phosphorus with frequency-resolved Raman spectroscopy. Journal of Applied Physics, 2018, 123, .  | 1.1 | 23        |
| 24 | Measurement of the thermal conductivities of suspended MoS <sub>2</sub> and MoSe <sub>2</sub> by nanosecond ET-Raman without temperature calibration and laser absorption evaluation. Nanoscale, 2018, 10, 23087-23102. | 2.8 | 51        |
| 25 | Nonmonotonic thickness-dependence of in-plane thermal conductivity of few-layered<br>MoS <sub>2</sub> : 2.4 to 37.8 nm. Physical Chemistry Chemical Physics, 2018, 20, 25752-25761.                                     | 1.3 | 45        |
| 26 | The hot carrier diffusion coefficient of sub-10 nm virgin MoS <sub>2</sub> : uncovered by non-contact optical probing. Nanoscale, 2017, 9, 6808-6820.   | 2.8 | 46        |
| 27 | A high-accuracy measurement method of glucose concentration in interstitial fluid based on microdialysis. Measurement Science and Technology, 2017, 28, 115701.   | 1.4 | 3         |
| 28 | Energy Transport State Resolved Raman for Probing Interface Energy Transport and Hot Carrier Diffusion in Few-Layered MoS <sub>2</sub> . ACS Photonics, 2017, 4, 3115-3129.   | 3.2 | 41        |
| 29 | Interfacial Thermal Conductance between Mechanically Exfoliated Black Phosphorus and<br>SiO <i><sub>x</sub></i> : Effect of Thickness and Temperature. Advanced Materials Interfaces, 2017, 4,<br>1700233.              | 1.9 | 16        |
| 30 | Identifying the Crystalline Orientation of Black Phosphorus by Using Optothermal Raman<br>Spectroscopy. ChemPhysChem, 2017, 18, 2828-2834.  | 1.0 | 12        |
| 31 | Asymmetry of Raman scattering by structure variation in space. Optics Express, 2017, 25, 18378.   | 1.7 | 4         |
| 32 | A continuous glucose monitoring device by graphene modified electrochemical sensor in microfluidic system. Biomicrofluidics, 2016, 10, 011910.  | 1.2 | 47        |
| 33 | A flexible electrochemical glucose sensor with composite nanostructured surface of the working electrode. Sensors and Actuators B: Chemical, 2016, 230, 801-809.  | 4.0 | 71        |
| 34 | Inkjet-printed microelectrodes on PDMS as biosensors for functionalized microfluidic systems. Lab on A Chip, 2015, 15, 690-695.   | 3.1 | 113       |
| 35 | A Method for Measuring the Volume of Transdermally Extracted Interstitial Fluid by a Three-Electrode<br>Skin Resistance Sensor. Sensors, 2014, 14, 7084-7095.   | 2.1 | 4         |